Effects of macitentan and tadalafil monotherapy or their combination on the right ventricle and plasma metabolites in pulmonary hypertensive rats

Argen Mamazhakypov[1] ©, Astrid Weiß[1], Sven Zukunft[2] ©, Akylbek Sydykov[1], Baktybek Kojonazarov[1], Jochen Wilhelm[1] ©, Christina Vroom[1], Aleksandar Petrovic[1], Djuro Kosanovic[1,3], Norbert Weissmann[1], Werner Seeger[1,4], Ingrid Fleming[2], Marc Iglarz[5], Friedrich Grimminger[1], Hossein A. Ghofrani[1], Soni S. Pullamsetti[1,4] and Ralph T. Schermuly[1]

[1]Cardio-Pulmonary Institute (CPI), Universities of Giessen and Marburg Lung Center, Member of the German Lung Center (DZL), Justus-Liebig-University Giessen, Giessen, Germany; [2]Institute for Vascular Signalling, Centre for Molecular Medicine, Goethe University, Frankfurt am Main, Germany & German Center of Cardiovascular Research (DZHK), Partner site RheinMain, Frankfurt am Main, Germany; [3]Sechenov First Moscow State Medical University (Sechenov University), Moscow, Russia; [4]Department of Lung Development and Remodelling, Max-Planck Institute for Heart and Lung Research, Bad Nauheim, Germany; [5]Actelion Pharmaceuticals Ltd, Allschwil, Switzerland

Abstract

Pulmonary arterial hypertension is a severe respiratory disease characterized by pulmonary artery remodeling. RV dysfunction and dysregulated circulating metabolomics are associated with adverse outcomes in pulmonary arterial hypertension. We investigated effects of tadalafil and macitentan alone or in combination on the RV and plasma metabolomics in SuHx and PAB models. For SuHx model, rats were injected with SU5416 and exposed to hypoxia for three weeks and then were returned to normoxia and treated with either tadalafil (10 mg/kg in chow) or macitentan (10 mg/kg in chow) or their combination (both 10 mg/kg in chow) for two weeks. For PAB model, rats were subjected to either sham or PAB surgery for three weeks and treated with above-mentioned drugs from week 1 to week 3. Following terminal echocardiographic and hemodynamic measurements, tissue samples were collected for metabolomic, histological and gene expression analysis. Both SuHx and PAB rats developed RV remodeling/dysfunction with severe and mild plasma metabolomic alterations, respectively. In SuHx rats, tadalafil and macitentan alone or in combination improved RV remodeling/function with the effects of macitentan and combination therapy being superior to tadalafil. All therapies similarly attenuated SuHx-induced changes in plasma metabolomics. In PAB rats, only macitentan improved RV remodeling/function, while only tadalafil attenuated PAB-induced changes in plasma metabolomics.

Introduction

Pulmonary arterial hypertension (PAH) is a severe disease characterized by pulmonary artery (PA) remodeling, leading to progressive increase in pulmonary vascular resistance (PVR), consequently resulting in right ventricular (RV) failure and premature death.[1] Various animal models of PAH have been developed to study molecular mechanisms underlying the disease as well as to examine the effects of potential therapeutics.[2] Among these models, monocrotaline (MCT) injection in rats and hypoxia exposure in mice and rats are most exploited.[3] However, in these models, animals do not

Corresponding author:
Ralph T. Schermuly, Universities of Giessen and Marburg Lung Center (UGMLC), Cardio-Pulmonary Institute (CPI), Aulweg 130, Giessen, 35392, Germany.
Email: ralph.schermuly@innere.med.uni-giessen.de

develop vasculopathy such as occlusive plexiform and concentric lesions that are observed in human PAH.[4] Combined use of the vascular endothelial growth factor receptor 2 (VEGFR2) inhibitor SU5416 and exposure to hypoxia (SuHx) in rats leads to severe PAH which closely mimics the vasculopathy observed in patients with PAH.[5] Importantly, in this model, rats develop severe maladaptive RV remodeling[6] which makes it preferential model to study pressure overload-induced RV remodeling. However, in SuHx rats, the changes in the RV are reflected by the changes in the pulmonary vasculature/hemodynamics, which limits SuHx model to study afterload-independent properties of the RV. This obstacle can be overtaken by employing pulmonary artery banding (PAB) model, which enables scientists to study direct, afterload-independent effects of potential therapeutics on the pressure overloaded RV.[7] Development of novel therapeutics targeting not only pulmonary vasculature but also the RV is crucial, since the survival of patients with PAH depends on the functional status of the RV.[8] Endothelin receptor antagonists (ERAs), phosphodiesterase type 5 (PDE5) inhibitors, prostanoids, and soluble guanylyl cyclase (sGC) stimulator are currently approved treatment strategies for PAH.[9] To achieve the maximum therapeutic effect using available approved agents, the concept of combination therapy has been proposed and in several clinical trials, the effects combination treatments were compared to monotherapy. The results of these trials showed that combination therapy is superior compared to monotherapy in the treatment of PAH patients.[10]

Endothelin-1 (ET-1) contributes to the development of PAH and some pharmacological agents targeting its receptors have been approved for the treatment of PAH such as ambrisentan, bosentan and macitentan.[9] However, the roles of ET-1 and its receptors in the pathogenesis of RV remodeling are poorly understood.[11] Macitentan is a dual ERA developed by modifying the chemical structure of bosentan to increase safety and efficacy,[12] which displays sustained receptor binding capacity and better tissue penetration.[13] The phase III clinical trial SERAPHIN showed that macitentan reduces morbidity and mortality, with improving pulmonary hemodynamics and 6-min walk distance (6MWD).[14] Furthermore, the effects of macitentan on two primary endpoints including RV stroke volume (RVSV) (measured by magnetic resonance imaging (MRI)) and pulmonary vascular resistance (PVR) (measured by right heart catheterization (RHC)) in PAH patients were studied as monotherapy or combination therapy with PDE5 inhibitors in the REPAIR multicentre study (ClinicalTrials.gov: NCT02310672). Analysis on 42 enrolled patients showed that at 26 weeks, both primary endpoints were met as shown by significantly increased RVSV for 15.2 ml and decreased PVR for 37% by macitentan.[15] Based on the positive results of this trial, enrolment was stopped in 42 patients and all enrolled patients will remain in the study up to their 52-week assessments. In addition, recent trials showed that

combination treatment with ERAs and PDE5 inhibitors improves RV remodeling and function in patients with scleroderma-associated PAH[16] as well as in IPAH patients.[17] However, the effects of these therapeutics on the RV have not been fully explored.

The mechanisms of RV remodeling in PAH are complex and various neurohormonal mediators contribute to the pathogenesis of pressure overload-induced RV remodeling.[18] In addition, preclinical studies have proved that dysregulated metabolism is also one of the underling mechanisms of RV failure.[19] In line with these findings, recent studies have shown that patients with PAH display dysregulated circulating metabolomics[20] and some of them are associated with disease outcome.[20]

In the present study, we aimed to investigate the development of RV remodeling/dysfunction in SuHx and PAB rats and the effects of PDE5 inhibitor tadalafil and a dual ERA macitentan alone or in combination on the RV. In addition, we employed targeted metabolomics to study; (1) if SuHx and PAB rats display changes in circulating metabolites and (2) if those changes can be corrected by tadalafil and macitentan alone or in combination.

Methods

Study approval

All experiments were conducted according to institutional guidelines complying with national and international regulations. All experimental procedures were approved by our University Animal Care Committee and the Federal Authorities for Animal Research. Animal studies are reported in compliance with the ARRIVE guidelines.[21]

Adult male Wistar-Kyoto rats (Janvier Labs, Saint Berthevin, France) with a body weight (BW) of 250–300 g were used and were provided free access to water and standard rat chow (Altromin #1324, Altromin, Lage, Germany) and were housed in a room with a 12:12-h light cycle, a temperature of 21 °C, and a humidity of 55%.

Chemicals

SU5416 (Tocris, Bristol, United Kingdom) was suspended in carboxymethylcellulose (CMC) solution (0.5% (wt/vol) carboxymethylcellulose sodium, 0.9% (wt/vol) NaCl, 0.4% (vol/vol) polysorbate, 0.9% (vol/vol) benzyl alcohol in deionized water). Macitentan and tadalafil (provided by Actelion Pharmaceuticals Ltd, Allschwil, Switzerland) were mixed in pulverized chow (Altromin #1324, Altromin, Lage, Germany) corresponding to a dose of 10 mg/kg/day.

SU5416/hypoxia exposure

Adult male Wistar-Kyoto rats were injected subcutaneously with the VEGFR2 inhibitor, SU5416 (20 mg/kg) under isoflurane anesthesia and exposed to chronic hypoxia

(10% oxygen) for three weeks (SuHx) and they were returned to normoxia for additional two weeks. From the day of returning to normoxia, rats were treated orally with 10 mg/kg/day tadalafil in chow ($n = 8$) or 10 mg/kg/day macitentan in chow ($n = 8$) or a combination of tadalafil and macitentan, both 10 mg/kg/day in chow ($n = 8$) or placebo ($n = 7$) for 14 days until the day of the final hemodynamic measurements. Rats injected with saline and kept at normoxia for 35 days were used as a healthy normoxic control group ($n = 4$).

Pulmonary artery banding surgery

Adult male Wistar-Kyoto rats (Janvier Labs, Saint Berthevin, France) weighing 250–300 g at the time of surgery were subjected to banding of the pulmonary artery trunk or sham operation under continuous anesthesia with 2–3% isoflurane mixed in 100% oxygen at flow rate of 1 L/min using an anesthesia system (Tabletop Laboratory Animal Anesthesia System, VetEquip Inc., Pleasanton, USA), and a subcutaneous administration of 0.05 mg/kg buprenorphine hydrochloride. Rats were intubated, and respiration was controlled by a small animal ventilator (SAR-830/A, CWE Inc., U.S.A.). Through left thoracotomy, a surgical thread (4–0 proline) was tied tightly around an 18-gauge needle alongside the pulmonary trunk. Then, the needle was rapidly removed creating a fixed constricted opening with the lumen equal to the diameter of the needle. The thorax was closed with vicryl suture. Sham-operated animals underwent the same surgical procedure without banding of the pulmonary trunk ($n = 8$). From 7th day of PAB, rats were treated orally with 10 mg/kg/day tadalafil in chow ($n = 9$) or macitentan with 10 mg/kg/day in chow ($n = 8$) or a combination of tadalafil and macitentan, both 10 mg/kg/day in chow ($n = 9$) or placebo ($n = 8$) for 14 days until the day of the final hemodynamic measurements.

Echocardiography

Echocardiography was performed with the VEVO2100 system equipped with a 13- to 24-MHz (MS250, rat cardiovascular) transducer (VisualSonics) in isoflurane anesthetized spontaneously breathing rats. All echocardiographic images were stored and were analyzed offline according to the software Vevo LAB. The following echocardiographic parameters were calculated: right ventricular internal diameter (RVID), right ventricular free wall thickness (RVWT), tricuspid annular plane systolic excursion (TAPSE), and cardiac output (CO) as described previously.[22–24]

Briefly, RVID was measured as the maximal distance from the RV free wall to the septum using the apical four-chamber view or parasternal long axis view. CO was calculated as the product of the velocity-time integral of the pulsed-Doppler tracing of either LV or RV outflow tract, the cross-sectional area of the LV or RV outflow tract, and the HR. Total pulmonary resistance (TPVR) was calculated using the following formula: TPVR = RVSP/CO, where RVSP is right ventricular systolic pressure (mmHg), and CO is the cardiac output (ml/min).

Hemodynamics

Rats were anesthetized in an anesthesia induction chamber supplied with 3–5% isoflurane mixed in 100% oxygen at a flow rate of 1 L/min delivered using an anesthesia system (Tabletop Laboratory Animal Anesthesia System, VetEquip Inc., Pleasanton, USA). Once rats were anesthetized and tracheotomy was performed, they were placed on a homeothermic plate (AD Instruments, Spechbach, Germany) and ventilated at a constant frequency of 60 breaths/min with a small animal ventilator (SAR-830/A, CWE Inc., U.S.A.) with maintained anesthesia of 1–2% isoflurane in 100% oxygen. The inspiratory time was 0.5 s and the positive end expiratory pressure (PEEP) was adjusted to 1 cm H_2O. 2-F Micro-Tip pressure catheters (SPR-320, Millar Instruments, Houston, Texas) were inserted into the left carotid artery to measure systolic systemic arterial pressure (SBP) or right jugular vein to measure right ventricular systolic pressure (RVSP).

Assessment of right ventricular hypertrophy

The heart was carefully dissected from the surrounding tissues and main arteries and veins. Right ventricle, septum and left ventricle were carefully separated from each other and wet weights were taken. RV hypertrophy (Fulton's Index) was calculated as the ratio of right ventricular weight/ (left ventricular weight + septum weight).

Histology of pulmonary artery muscularization

The formalin-fixed lungs were subject to paraffin embedding. The paraffin-embedded tissues were cut to 3 μm thick sections. The degree of muscularization of small pulmonary arteries was assessed by double-staining the 3 μm sections with an anti-α-smooth muscle actin (α-SMA) antibody and anti-von Willebrand factor (vWF) antibody. The analysis of the vessels was performed using a computerized morphometric analysis system (QWin; Leica, Wetzlar, Germany) to determine the degree of pulmonary artery muscularization. In each rat, around 100 arteries with diameters of 20 to 70 μm were analyzed and each artery was categorized as non-muscularized, partially muscularized or fully muscularized.

Assessment of right ventricular fibrosis

Freshly dissected right ventricular tissue was fixed in 4% paraformaldehyde overnight, then dehydrated and embedded in paraffin and sectioned at a thickness of 3 μm. To evaluate collagen fiber deposition, RV sections were stained with 0.1% Sirius Red (Sirius Red F3B, Niepoetter,

Bürstadt, Germany) in picric acid (Fluka, Neu-Ulm, Germany). Photomicrographs were quantified to determine the collagen fraction using Leica Qwin V3 computer-assisted image analysis software (Leica Microsystem, Wetzlar, Germany).

Real-time polymerase chain reaction

Total mRNA was extracted from frozen rat right ventricular tissue samples with the RNeasy Mini Kit (Qiagen). For cDNA synthesis, 1 μg of total RNA sample was used per 20 μl cDNA reaction. cDNA was synthesized using iScript cDNA synthesis kit (Bio-Rad) and T3000 Thermocycler (Biometra, Göttingen, Germany). qPCR was then performed with the iQ SYBR Green Supermix (Bio-Rad) kit. The primers used for real-time quantitative PCR are presented in the Supplementary Table 1. Expression was analyzed with the ΔCt method. The Ct values of the target genes were normalized to that of the housekeeping gene (endogenous control) encoding porphobilinogen deaminase (PBGD) using the equation ΔCt = Ctreference – Cttarget and expressed as ΔCt.

Circulating NT-proBNP measurements

Plasma levels of N-terminal pro-B-type natriuretic peptide (NT-proBNP) were measured by the ELISA Kit specific for rats.

Targeted metabolomics

Whole blood was collected in EDTA tubes by right ventricular puncture following terminal hemodynamics measurements. Plasma was separated from erythrocytes by centrifugation. Further, samples were stored frozen

($-80\,^{\circ}$C) until metabolite extraction. The endogenous metabolites were analyzed in 10 μl of plasma samples using the Biocrates Absolute-IDQ P180 kit (BIOCRATES, Life Science AG, Innsbruck, Austria) which combines direct flow injection analysis (FIA) and liquid chromatography (LC) coupled to tandem mass spectrometry (MS/MS) assay as described previously.[25] The sample preparation and measurements were performed according to the manufacturers' manual of the p180 kit (UM-P180). Following extraction and derivatization, amino acids and biogenic amines were detected and quantified by LC coupled to MS/MS, while other metabolites were analyzed using FIA coupled to MS/MS on AB SCIEX 4000 QTrapTM mass spectrometer (AB SCIEX, Darmstadt, Germany) equipped with a 1200 Series HPLC (Agilent Technologies Deutschland GmbH) and an HTC PAL auto sampler (CTC Analytics) controlled with use of the software Analyst 1.5. The method allows to detect a total of 186 annotated metabolites including 41 amino acids and biogenic amines, 40 acylcarnitines (Cx:y), hydroxyacylcarnitines (C (OH) x:y) and dicarboxylacylcarnitines (Cx:y-DC), the sum of hexoses (one resultant metabolite), 15 sphingomyelins (SMx:y) and sphingomyelin derivatives (SM (OH) x:y) as well as 90 glycerophospholipids (14 lyso-phosphatidylcholines (lysoPC) and 75 phosphatidylcholines (PC)). Analyzed glycerophospholipids are further subclassified into an ester ("a") or an ether ("e") types according to the chemical linkage of the fatty chain at the sn-1 or sn-2 position of glycerol backbone. The two letters "aa" (=diacyl) and "ae" (=acyl-alkyl) designate that two fatty acid residues are bound to glycerol, while a single letter "a" (= acyl) designate presence of a single fatty acid residue. The lipid side chain composition is abbreviated with "Cx:y", where "x" symbolize the number of carbons in the side chain and "y" the number of double bonds. In addition,

Table 1. Characteristics of SuHx rats.

Parameters	Control	SuHx Placebo	SuHx Tadalafil	SuHx Macitentan	SuHx combination
N	4	7	8	8	8
BW (g)	357.8 ± 9.0	**266.8 ± 7.7**	326.8 ± 3.9	**339.6 ± 5.0**	**339.3 ± 6.1**
SBP (mmHg)	72.7 ± 3.1	**58.2 ± 1.0**	59.8 ± 2.3	60.6 ± 1.5	59.4 ± 2.2
HR (bpm)	277 ± 2.2	270 ± 9.1	260 ± 11.7	262 ± 7.2	265 ± 6.9
RVSP (mmHg)	25.1 ± 2.5	**57.6 ± 3.8**	**42.8 ± 3.0**	**29.3 ± 1.1**	**26.1 ± 0.6**
CO (mL/min)	85.5 ± 1.4	**48.6 ± 3.7**	**74.4 ± 3.8**	**84.6 ± 5.0**	**90.3 ± 3.3**
TPVR (mmHg/ml/min)	0.30 ± 0.03	**1.23 ± 0.14**	**0.58 ± 0.05**	**0.35 ± 0.02**	**0.29 ± 0.01**
RVID (mm)	3.34 ± 0.13	**5.07 ± 0.13**	**4.44 ± 0.13**	**4.33 ± 0.13**	**4.01 ± 0.20**
TAPSE (mm)	2.68 ± 0.09	**1.56 ± 0.08**	**1.97 ± 0.04**	**2.37 ± 0.09**	**2.59 ± 0.09**
RV/(LV+S)	0.26 ± 0.01	**1.42 ± 0.02**	**0.51 ± 0.02**	**0.41 ± 0.01**	**0.35 ± 0.01**

Note: All parameters are expressed as mean ± standard error of mean (SEM). Differences assessed by one-way ANOVA and Tukey's multiple comparison test; values in bold fonts, $p \leq 0.05$ for SuHx placebo compared to sham, for SuHx treatment groups compared to SuHx placebo.
N: number; SuHx: SU5416 injection plus hypoxia exposure; BW: body weight; RVSP: right ventricular systolic pressure; HR: heart rate; SBP: systolic blood pressure; CO: cardiac output; CI: cardiac index; TPVR: total pulmonary vascular resistance; RVID: right ventricular internal diameter; TAPSE: tricuspid annulus systolic excursion; RV/(LV + S): the ratio of right ventricular mass divided by left ventricular mass plus septum mass.

29 metabolite ratios with known biological functions were analyzed. Metabolite concentrations are reported in µM units.

Statistical analysis of the data

All results were shown as the mean ± standard error of the mean (SEM) unless otherwise indicated. Data were plotted as individual data points with mean in addition. The different groups were compared using one-way analysis of variance (ANOVA) and subsequent application of Tukey post hoc analysis. A p value less than 0.05 was considered statistically significant. In the figures, asterisks denote achieved levels of statistical significance (*$p < 0.05$; **$p < 0.01$; ***$p < 0.001$; ****$p < 0.0001$). For some variables such as NT-proBNP levels and RV fibrosis, we performed log transformation (for TN-proBNP) or logit transformation (for RV fibrosis) before statistical testing to approximate normal distribution with equal variances. All statistical analyses were performed with the use of Graphpad Prism 7 (Graphpad Software, La Jolla, CA, USA).

Metabolites were analyzed using Metaboanalyst 4.0 software. We excluded metabolite species with more than 50% missing values. The remaining missing values and zeros were replaced by the half of the minimum positive value of the respective metabolite. Log2 transformed metabolite values were used for the analysis. Comparisons of metabolites/metabolite ratios between groups were done using

ANOVA followed by Tukey post hoc analysis. All p-values were adjusted for multiple testing using Benjamini-Hochberg false discovery rate correction (FDR) and FDR ≤ 0.05 was used as a significance threshold (q-values). We performed an exploratory analysis of the data by sparse partial least squares-discriminant analysis (sPLS-DA) to see if the data were capable to separate the groups under investigation based on their metabolomics profile. Heatmaps were generated based on the most altered metabolites between disease model and control animals. The pathway analysis was performed to identify the most relevant pathways representing the disturbed metabolites.

Results

Therapeutic effects on cardio-pulmonary function in SuHx rats

SuHx rats were randomly assigned to different treatment groups (placebo, tadalafil, macitentan and a combination of tadalafil and macitentan) for two weeks upon returning to normoxia after SU5416 injection and hypoxia exposure for three weeks. All rats survived until the end of the study (35 days). In all studied groups, rats had similar values of heart rate (HR) (Fig. 1a). SuHx rats from all groups had significantly decreased systemic systolic blood pressure (SBP) compared to normoxia control rats and none of the applied treatments further changed SBP values (Fig. 1b).
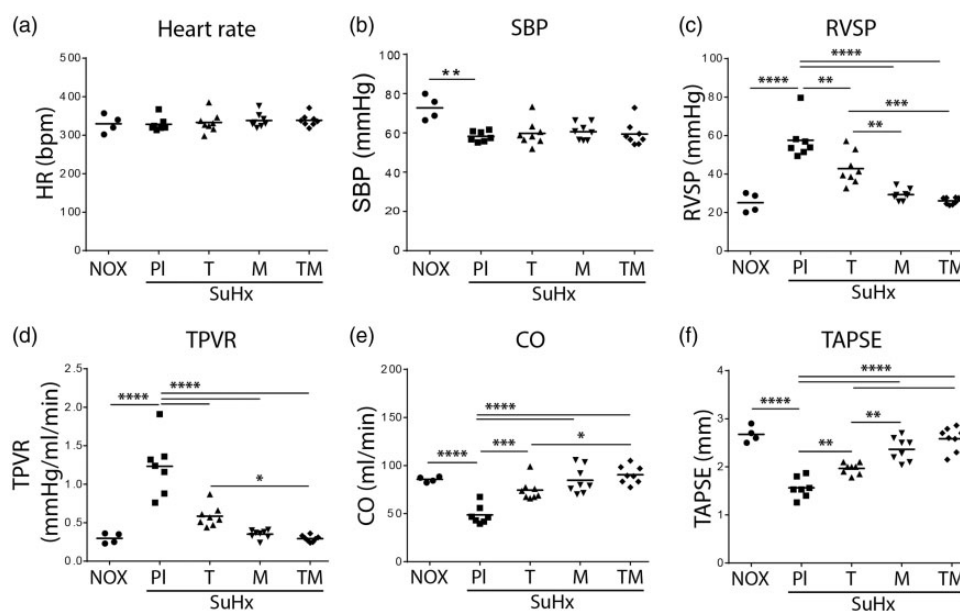
Fig. 1. Effects of tadalafil, macitentan, or their combination on hemodynamics and cardiac function in SuHx rats. (a) Heart rate (HR, bpm); (b) Systemic systolic blood pressure (SBP, mmHg); (c) Right ventricular systolic pressure (RVSP, mmHg); (d) Total pulmonary vascular resistance (TPVR, mmHg/mL/min); (e) Cardiac output (CO, mL/min); (f) Tricuspid annulus plane systolic excursion (TAPSE, mm). NOX: normoxic control ($n = 4$), SuHx: SU5416 plus hypoxia; Pl: placebo ($n = 7$); T: tadalafil ($n = 8$); M: macitentan ($n = 8$); TM: combination of tadalafil and macitentan ($n = 8$). Data are given as scatter dot plots, and lines are means. Differences assessed by one-way ANOVA and Tukey's multiple comparison test; *$p = 0.05$, **$p = 0.01$, ***$p = 0.001$, ****$p = 0.0001$.

Five weeks after SU5416 injection, hemodynamics and echocardiographic measurements revealed that placebo SuHx rats developed severe PAH as evidenced by significantly increased RVSP (Fig. 1c) and TPVR (Fig. 1d) compared to control rats (Table 1). Elevated RVSP was associated with significantly compromised RV function as shown by decreased CO (Fig. 1e) and TAPSE (Fig. 1f) in placebo SuHx rats compared to control rats (Table 1). Moreover, SuHx rats developed severe RV remodeling as shown by increased RV dilatation (RVID) (Fig. 2a) and RV hypertrophy index (RV/LV + S) (Fig. 2b) compared to control rats (Table 1).

Therapy with tadalafil and macitentan alone or in combination for two weeks significantly reduced RVSP (Fig. 1c) in parallel with reduced TPVR (Fig. 1d) compared with placebo SuHx rats (Table 1). Next, tadalafil and macitentan alone or in combination significantly improved RV function as shown by increased cardiac output (CO) (Fig. 1e) and TAPSE (Fig. 1f) compared to placebo SuHx rats (Table 1). Remarkably, TAPSE values indicated that RV function improved significantly better with both macitentan and combination therapy compared to tadalafil (Fig. 1f, Table 1). Additionally, RV dilatation (RVID) was significantly improved after treatment with tadalafil and macitentan alone or in combination (Fig. 2a) with the latter having greater effect. Although, all therapies significantly reduced RV hypertrophy (RV/LV+S) as compared with placebo (Fig. 2b), more pronounced RV reverse-hypertrophy effect was noticed with macitentan and combination therapy compared to tadalafil (Fig. 2b). In addition, placebo SuHx rats displayed significant increase in RV fibrosis compared to control rats (Fig. 2c and e) and none of the therapies decreased RV fibrosis (Fig. 2c and e). Moreover, placebo SuHx rats displayed increased circulating levels of N-terminal pro B-type natriuretic peptide (NT-proBNP) (Fig. 2d), and tadalafil and macitentan alone or in combination attenuated these changes in SuHx rats (Fig. 2d). Importantly, the development of RV failure in placebo SuHx rats was also accompanied with significantly increased expressions of cardiac hypertrophy markers such as A-type natriuretic peptide precursor (NPPA) and B-type natriuretic peptide precursor (NPPB) (Fig. 2f). Although, collagen type I alpha 1 chain (Col1A1) expression was not changed significantly, the expression of collagen type III alpha one chain (Col3A1) was significantly increased in the RV myocardium of placebo SuHx rats compared to that of sham rats (Fig. 2f). Treatment with tadalafil and macitentan alone or in combination corrected NPPA and NPPB expressions. However, the expression of Col1A1 was attenuated with macitentan and combination treatment, while Col3A1 expression was reduced only with combination treatment (Fig. 2f).

Placebo SuHx rats developed severe PA remodeling as evidenced by marked increase in the proportion of fully muscularized arteries (Fig. 2g), however, without significant changes in the proportions of non-muscularized and partially muscularized arteries (Fig. 2g). Among therapies with tadalafil and macitentan alone or in combination, only the latter significantly decreased the percentage of muscularized vessels compared to placebo (Fig. 2g).

Therapeutic effects on cardio-pulmonary function in PAB rats

PAB-operated rats were randomly assigned to either placebo or tadalafil or macitentan or their combination for two weeks after day 7 of PAB surgery (Table 2). Rats from all groups survived till the end of the study (21 days). PAB rats from all groups had similar levels of heart rate (HR) (Fig. 3a) as well as systemic systolic blood pressure (SBP) values (Fig. 3b, Table 2). At 21st day after PAB surgery, hemodynamics and echocardiographic measurements showed that placebo-treated PAB rats developed severe increase in RVSP (Fig. 3c) accompanied with decreased CO (Fig. 2d). In addition, TAPSE was also reduced in placebo PAB rats compared to sham rats (Fig. 3e). Moreover, PAB rats developed RV remodeling as shown by increased RV dilatation (RVID) (Fig. 4a), RV wall thickness (RVWT) (Fig. 4b) and RV hypertrophy (RV/(LV+S)) (Fig. 4c) as compared to sham rats. Therapies with tadalafil and macitentan alone or in combination for two weeks did not significantly change the values of RVSP compared with placebo PAB rats (Fig. 3c). Next, among treatment groups only macitentan improved RV function as shown by increased TAPSE (Fig. 4e) compared to placebo PAB rats. Additionally, only macitentan significantly reduced RVID as compared with placebo (Fig. 4a). Similarly, RV hypertrophy also was improved significantly only with macitentan (Figure 4(c)) as compared to placebo PAB rats (Figure 4(a)). In addition, RV fibrosis was increased in PAB rats compared to sham rats (Figure 4(d) and (f)); however, none of the therapies decreased RV fibrosis significantly compared to placebo PAB rats (Figure 4(d) and (f)). Similarly, circulating NT-proBNP levels were also significantly increased in placebo PAB rats and none of the therapies further decreased its levels in PAB rats (Fig. 4e). RV remodeling in PAB rats was associated with significantly increased expressions of cardiac hypertrophy markers such as NPPA, NPPB and Col3A1 (Fig. 4g) and none of the therapies attenuated their expressions (Fig. 4g).

Metabolite dynamics in SuHx and PAB rats

We exploited targeted metabolomics profiling to investigate the changes of plasma metabolites in both SuHx and PAB models. In our study, out of 186 detectable metabolites, 140 (75%) were detected in each study group. Additionally, we investigated the behavior of metabolite ratios which serve as markers for known biological functions. From the 29 ratios, 27 were analyzed in each group. sPLS-DA indicates that placebo SuHx rats were separated from healthy control rats, macitentan- and combination-treated SuHx rats
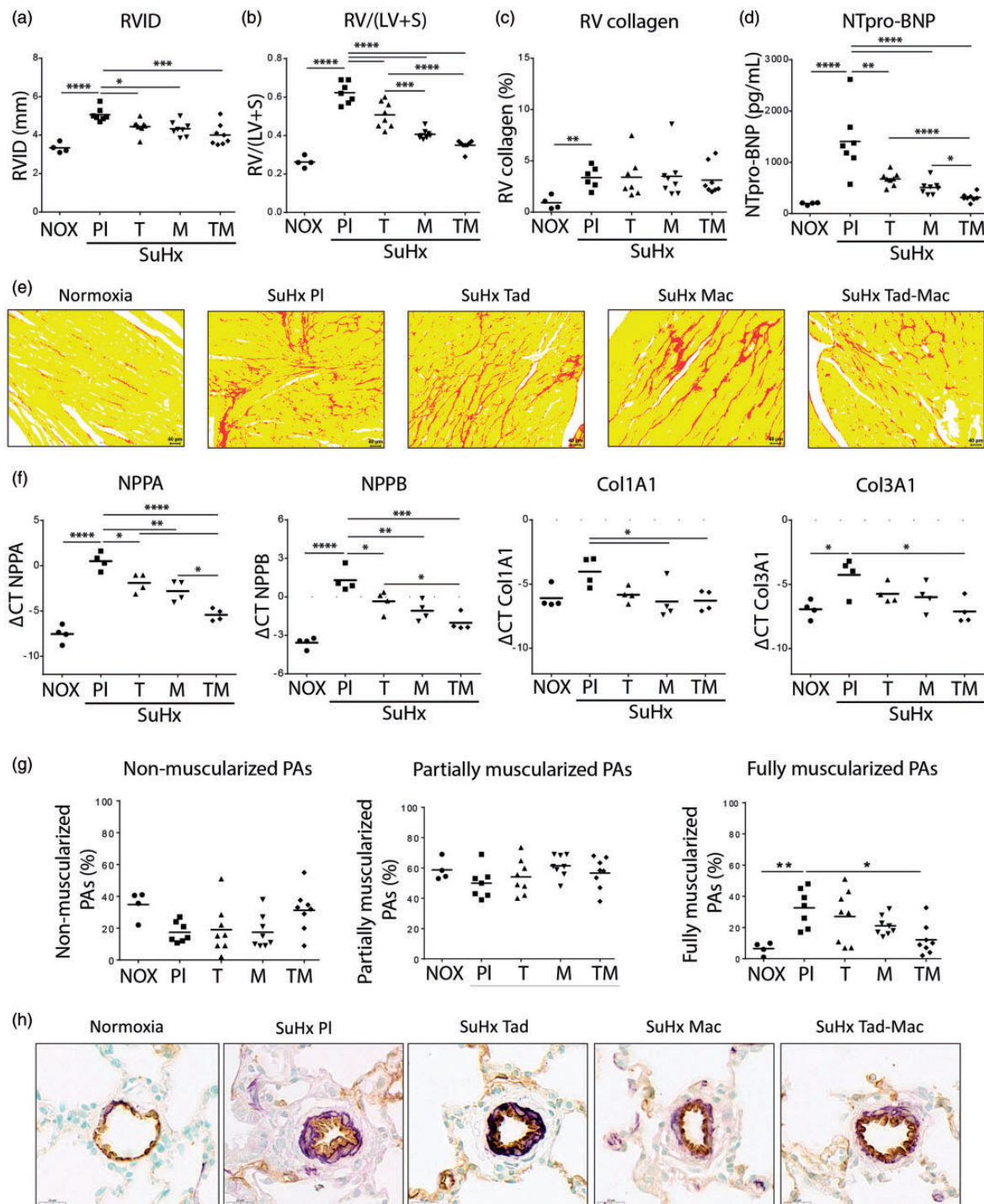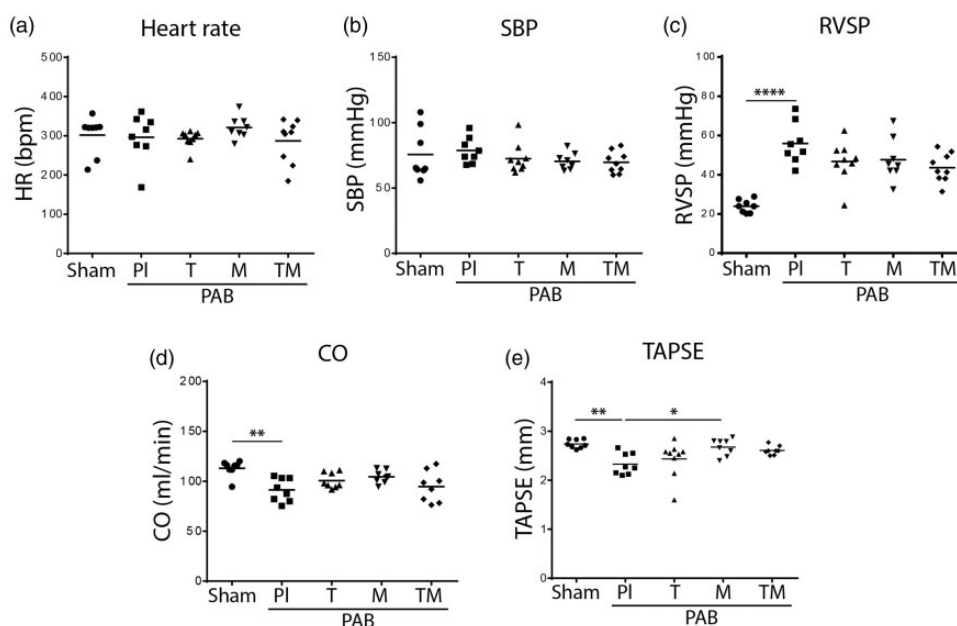
Fig. 2. Effects of tadalafil, macitentan, or their combination on the right ventricular and pulmonary artery remodeling in SuHx rats. (a) Right ventricular internal diameter (RVID) (mm); (b) Ratio of the right ventricular (RV) mass to left ventricular (LV) and septum (S) mass (RV/LV + S); (c) Right ventricular collagen area (RV collagen area, %); (d) Circulating blood plasma concentration of N-terminal pro brain natriuretic peptide (NT-proBNP) (pg/mL); (e) Representative images of sirius red staining for collagen visualization. Scale bar: 20 μm. (f1) A-type natriuretic peptide precursor (NPPA) mRNA expression in right ventricular (RV) tissue homogenate; (f2) B-type natriuretic peptide precursor (NPPB) mRNA expression in right ventricular (RV) tissue homogenate; (f3) collagen type I alpha 1 chain (Col1A1) mRNA expression in right ventricular (RV) tissue homogenate; (f4) expression of collagen type III alpha 1 chain (Col3A1) mRNA expression in right ventricular (RV) tissue homogenate. (g) The proportion of non-muscularized, partially muscularized and fully muscularized pulmonary arteries (diameter 25–50 μm) was determined via immunohistology staining of lung sections for vWF (brown) and α-SMA (violet) together with methylgreen for counterstaining. (h) Representative images for all five study groups are shown. Scale bar: 20 μm. NOX: normoxic control ($n = 4$); SuHx: SU5416 plus hypoxia; Pl: placebo ($n = 7$); T: tadalafil ($n = 8$); M: macitentan ($n = 8$); TM: combination of tadalafil and macitentan ($n = 8$). SuHx: sugen plus hypoxia; Pl: placebo; T: tadalafil; M: macitentan; TM: combination of tadalafil and macitentan. Differences assessed by one-way ANOVA and Tukey's multiple comparison test; *$p = 0.05$, **$p = 0.01$, ***$p = 0.001$, ****$p = 0.0001$.

Table 2. Characteristics of PAB rats.

Parameters	Sham	PAB Placebo	PAB Tadalafil	PAB Macitentan	PAB Combination
N	8	8	9	8	9
BW (g)	319.4 ± 3.92	316.6 ± 3.22	**342.8 ± 3.60**	**342.0 ± 4.40**	319.3 ± 10.13
SBP (mmHg)	75.6 ± 6.8	78.7 ± 3.5	72.5 ± 3.7	70.4 ± 2.3	69.7 ± 2.7
HR (bpm)	302 ± 17.4	296 ± 21.3	293 ± 7.25	321 ± 10.0	287 ± 18.4
RVSP (mmHg)	24.0 ± 1.2	**55.9 ± 3.7**	46.8 ± 3.4	47.7 ± 3.8	43.6 ± 2.5
CO (mL/min)	113 ± 2.8	**91.3 ± 4.2**	100.7 ± 2.7	104.5 ± 2.3	94.8 ± 5.5
TAPSE (mm)	2.74 ± 0.03	**2.33 ± 0.08**	2.43 ± 0.12	**2.67 ± 0.06**	2.61 ± 0.03
RVID (mm)	1.62 ± 0.05	**2.43 ± 0.12**	2.40 ± 0.13	**1.95 ± 0.05**	2.11 ± 0.10
RV/(LV + S)	0.29 ± 0.01	**0.57 ± 0.03**	0.51 ± 0.02	**0.45 ± 0.02**	0.48 ± 0.03

Note: All parameters are expressed as mean $\pm$ standard error of mean (SEM). Differences assessed by one-way ANOVA and Tukey's multiple comparison test; values in bold fonts, $p \leq 0.05$ for SuHx placebo compared to sham, for SuHx treatment groups compared to SuHx placebo.
PAB: pulmonary artery banding; BW: body weight; RVSP: right ventricular systolic pressure; HR: heart rate; SBP: systolic blood pressure; CO: cardiac output; RVID: right ventricular internal diameter; TAPSE: tricuspid annulus systolic excursion; RV/(LV+S): the ratio of right ventricular mass divided by left ventricular mass plus septum mass.
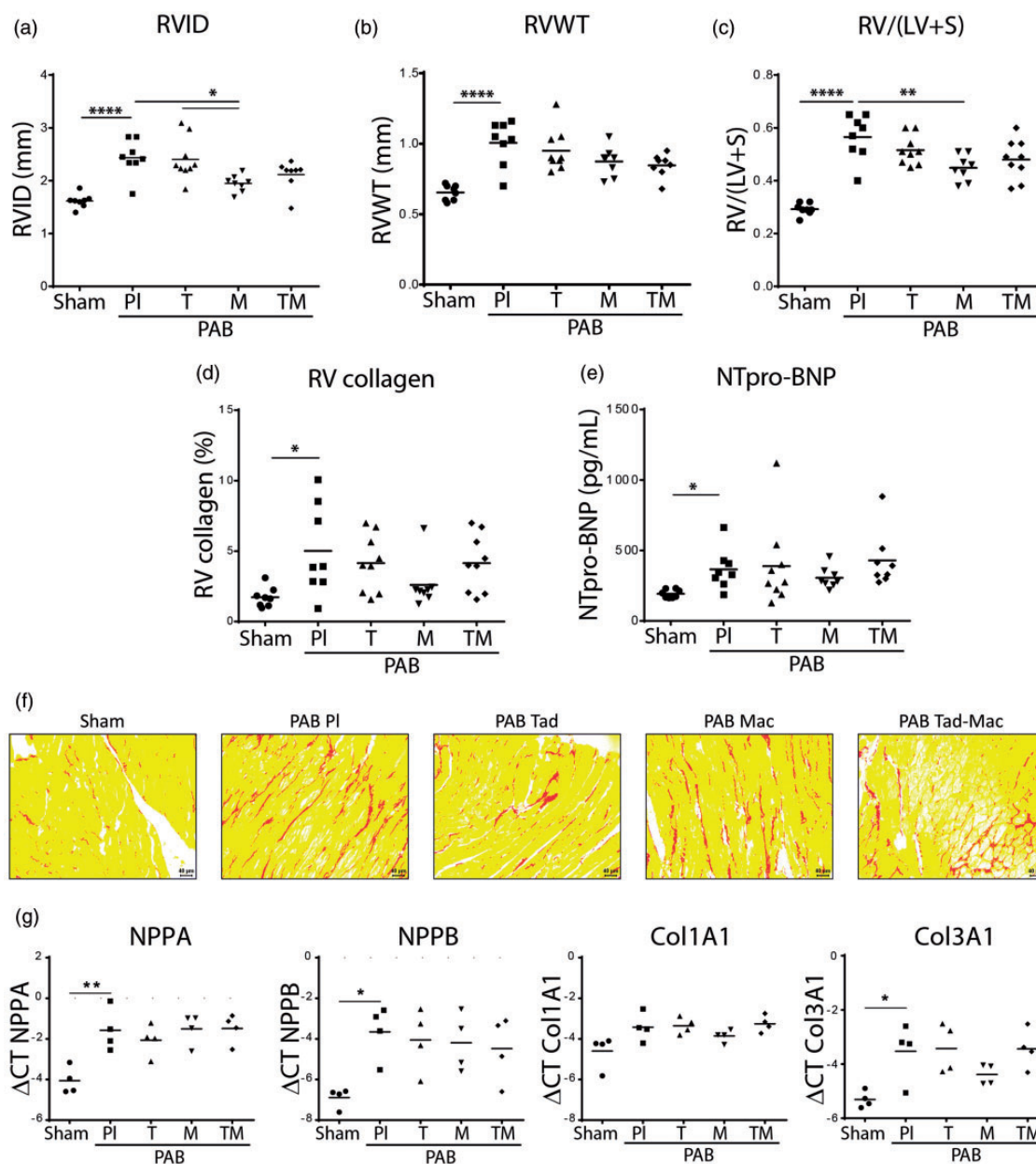

Fig. 3. Effects of tadalafil, macitentan, or their combination on systemic and pulmonary hemodynamics and cardiac function in PAB rats. (a) Heart rate (HR, bpm); (b) Systemic systolic blood pressure (SBM, mmHg); (c) Right ventricular systolic pressure (RVSP, mmHg); (d) Cardiac output (CO, mL/min); (e) Tricuspid annulus plane systolic excursion (TAPSE, mm). Sham ($n = 8$); PAB: pulmonary artery banding; Pl: placebo ($n = 8$); T: tadalafil ($n = 9$); M: macitentan ($n = 8$); TM: combination of tadalafil and macitentan ($n = 8$). Differences assessed by one-way ANOVA and Tukey's multiple comparison test; *$p = 0.05$, **$p = 0.01$, ***$p = 0.001$, ****$p = 0.0001$.

(Fig. 5a). Among the treated groups, macitentan- and combination-treated SuHx rats overlapped with healthy control rats. In contrast, tadalafil-treated SuHx rats displayed some overlapping with placebo-treated SuHx rats but not with healthy control rats (Fig. 5a). Then, we investigated the changes, which were significantly different between placebo SuHx rats versus healthy normoxia control rats. From 167 metabolites/metabolite ratios, 25 were significantly altered in placebo SuHx rats compared to healthy normoxia control rats (FDR < 0.05) (Fig. 5b); 18 metabolites and 7 metabolite ratios (Table 3). These disturbed metabolites included phosphatidylcholines (PC aa C34:1, PC ae C36:5, PC ae C38:4, PC ae C42:1, PC aa C32:1, PC ae C34:1, PC aa C36:1, PC ae C36:1, PC ae C36:3, PC aa C36:2, and PC aa C34:3), lysophosphatidylcholines (LysoPC a C20:3, LysoPC a C17:0, LysoPC a C28:0), fatty acylcarnitines (C18:1 and C16:1), sphingophospholipids (SM (OH) C14:1) and biogenic amines (Ac-Orn). Abnormal metabolite ratios included

Fig. 4. Effects of tadalafil, macitentan, or their combination on the right ventricular hypertrophy in PAB rats. (a) Right ventricular internal diameter (RVID, mm); (b) right ventricular wall thickness (RVWT, mm); (c) ratio of the right ventricular (RV) mass to left ventricular (LV) and septum (S) mass (RV/LV+S); (d) right ventricular collagen area (RV collagen area, %); (e) circulating blood plasma concentration of N-terminal pro brain natriuretic peptide (NT-proBNP, pg/mL); (f) Representative images of sirius red staining for collagen visualization. Scale bar: 20 μm. (g1) A-type natriuretic peptide precursor (NPPA) mRNA expression in right ventricular (RV) tissue homogenate; (g1) B-type natriuretic peptide precursor (NPPB) mRNA expression in right ventricular (RV) tissue homogenate; (g3) collagen type I alpha 1 chain (Col1A1) mRNA expression in right ventricular (RV) tissue homogenate; (g4) expression of collagen type III alpha 1 chain (Col3A1) mRNA expression in right ventricular (RV) tissue homogenate. Sham (n = 8); PAB: pulmonary artery banding; Pl: placebo (n = 8); T: tadalafil (n = 9); M: macitentan (n = 8); TM: combination of tadalafil and macitentan (n = 8). Differences assessed by one-way ANOVA and Tukey's multiple comparison test; *p = 0.05, **p = 0.01, ***p = 0.001, ****p = 0.0001.

MUFA PC/SFA PC, (C16+C18)/C0, Cit/Orn, Met-So/Met, PC aa/PC ae, Cit/Arg, and BCAA/aromatic AA (Table 3). Among 18 dysregulated metabolites, 6 metabolites were found to be significantly downregulated, whereas 12 metabolites were upregulated in the SuHx rats compared to healthy normoxia rats (Table 3). Although, tadalafil and macitentan alone or in combination attenuated most of the SuHx-induced changes in plasma metabolites/metabolite ratios. There were differences in metabolites exclusively attenuated by either tadalafil (PC aa C36:1, PC aa C36:3, (C16+C18)/C0, and BCAA/aromatic AA) or macitentan (LysoPC aC17:0, PC ae C84:4, PC ae C42:1, SM (OH)
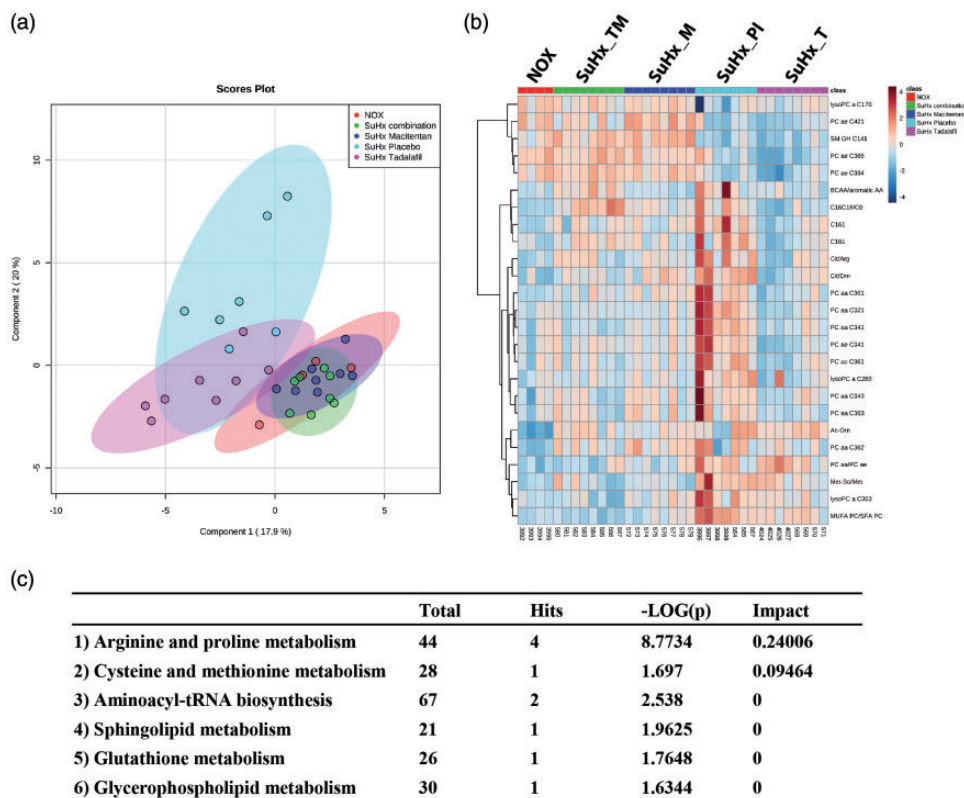
Fig. 5. Metabolomics profiling of plasma from SuHx rats. (a) metabolic profiling reveals clear separation between plasma metabolite profiles from SuHx placebo or tadalafil treated, versus combination, macitentan or healthy NOX rats by sparse partial least squares discriminant analysis; (b) heat map of top 25 significantly altered metabolites by the model ordered by hierarchical clustering. Each rectangle represents a metabolite colored by its normalized intensity scale. Red represents high, and blue represents low abundance of the metabolite relative to the mean (white); (c) six most effected pathways. NOX: normoxic control (n = 4); SuHx: SU5416 plus hypoxia; PI: placebo (n = 7); T: tadalafil (n = 8); M: macitentan (n = 8); TM: combination of tadalafil and macitentan (n = 8).

C14:1, and Met-So/Met) (Table 3). The pathway analysis shows that five pathways that most closely represented differences in metabolites/metabolite ratios between SuHx placebo and healthy normoxia groups were arginine/proline, cysteine/methionine, aminoacyl-tRNA biosynthesis, sphingolipid, glutathione and glycerophospholipid metabolisms; arginine/proline metabolism being the topmost altered pathway (Fig. 5c).

The same methodological and statistical approaches have been used to analyze plasma metabolites in PAB rats. Briefly, the sPLS-DA poorly separated placebo PAB rats from the sham rats. The tadalafil-treated PAB rats largely overlapped with these two groups, while macitentan- and combination-treated PAB rats showed only some overlapping with the other three groups (Fig. 6a). First, the significant changes between placebo PAB and sham rats were investigated. In total, from 167 metabolites/metabolite ratios detected, only three metabolite ratios were changed in PAB rats compared to sham rats (FDR < 0.05), which included (C2+C3)/C0, C2/C0 and (C16+C18)/C0 (Table 4). Among therapies, only tadalafil could significantly attenuate those changes in PAB rats. However, heatmap in Fig. 6b shows that there were more metabolites

profoundly altered due to combination treatment compared to other groups.

Discussion

In our study, we evaluated plasma metabolite profiles in SuHx and PAB rat models of RV remodeling. In addition, we studied the effects of tadalafil and macitentan alone or in combination on the RV and plasma metabolites in those models.

For the current study, doses of tadalafil and macitentan were selected based on a pilot dose–response experiment in SuHx rats equipped with telemetry. Our goal was to set experimental conditions allowing us to evaluate a possible additive effect of the combination. The telemetry data show that both tadalafil and macitentan at 10 mg/kg decrease mPAP for ≈20 mmHg from a baseline mPAP of ≈80 mmHg (data not shown), thus allowing some room to study any additive effect of the combination. In addition, the doses selected are in line with the most of preclinical studies that have investigated these compounds in PAH models: Tadalafil 10 mg/kg has been shown to be effective in various PAH models, in combination with ERAs

Table 3. The most dysregulated metabolites in SuHx rats, and effects of tadalafil and macitentan and their combination on these metabolites.

N	NOX 4	SuHx Placebo 7	SuHx Tadalafil 8	SuHx Macitentan 8	SuHx combination 8
Metabolites					
C16:1 (μM)	0.0335 ± 0.001	**0.0480 ± 0.004**	**0.0355 ± 0.002**	**0.0384 ± 0.001**	0.0381 ± 0.002
C18:1 (μM)	0.067 ± 0.004	**0.102 ± 0.012**	**0.067 ± 0.004**	**0.074 ± 0.003**	0.083 ± 0.003
Ac-Orn (μM)	3.53 ± 0.196	**7.87 ± 1.104**	8.07 ± 0.369	6.85 ± 0.288	7.33 ± 0.510
lysoPC a C17:0 (μM)	4.89 ± 0.325	**3.36 ± 0.416**	4.05 ± 0.136	**4.65 ± 0.108**	**4.45 ± 0.174**
lysoPC a C20:3 (μM)	1.07 ± 0.055	**2.34 ± 0.480**	**1.32 ± 0.090**	**1.33 ± 0.090**	**0.98 ± 0.097**
lysoPC a C28:0 (μM)	0.18 ± 0.016	**0.30 ± 0.046**	**0.20 ± 0.028**	**0.20 ± 0.008**	**0.19 ± 0.007**
PC aa C32:1 (μM)	1.98 ± 0.213	**5.69 ± 1.504**	**1.81 ± 0.223**	**2.00 ± 0.132**	**1.94 ± 0.079**
PC aa C34:1 (μM)	31.88 ± 2.943	**51.60 ± 6.159**	**32.40 ± 1.674**	**34.06 ± 1.164**	**30.65 ± 1.258**
PC aa C34:3 (μM)	3.61 ± 0.482	**6.49 ± 1.511**	3.96 ± 0.275	4.52 ± 0.258	3.98 ± 0.289
PC aa C36:1 (μM)	9.10 ± 0.188	**16.34 ± 2.595**	**9.66 ± 0.628**	11.76 ± 0.507	**10.69 ± 0.552**
PC aa C36:2 (μM)	77.73 ± 1.953	**101.9 ± 8.460**	92.69 ± 2.760	102.2 ± 3.108	95.29 ± 3.164
PC aa C36:3 (μM)	27.93 ± 2.135	**41.99 ± 7.107**	**27.30 ± 0.906**	32.90 ± 1.899	30.23 ± 1.913
PC ae C34:1 (μM)	2.24 ± 0.189	**3.28 ± 0.389**	**1.99 ± 0.106**	**2.41 ± 0.084**	**2.42 ± 0.089**
PC ae C36:1 (μM)	1.29 ± 0.113	**1.88 ± 0.200**	**1.23 ± 0.072**	**1.36 ± 0.051**	**1.33 ± 0.069**
PC ae C36:5 (μM)	1.81 ± 0.079	**1.46 ± 0.101**	1.20 ± 0.055	1.67 ± 0.046	**1.77 ± 0.055**
PC ae C38:4 (μM)	10.62 ± 0.808	**7.63 ± 0.477**	6.67 ± 0.599	**10.46 ± 0.401**	**10.83 ± 0.332**
PC ae C42:1 (μM)	0.73 ± 0.056	**0.49 ± 0.041**	0.47 ± 0.023	**0.76 ± 0.039**	0.61 ± 0.036
SM (OH) C14:1 (μM)	0.81 ± 0.055	**0.63 ± 0.032**	0.61 ± 0.034	**0.99 ± 0.042**	**0.91 ± 0.038**
Metabolite ratios					
(C16 + C18)/C0	0.004 ± 0.000	**0.006 ± 0.001**	**0.004 ± 0.000**	0.005 ± 0.000	0.007 ± 0.001
Cit/Arg	0.38 ± 0.022	**0.66 ± 0.077**	**0.42 ± 0.033**	**0.47 ± 0.014**	0.49 ± 0.030
Cit/Orn	1.02 ± 0.102	**1.74 ± 0.110**	**1.18 ± 0.076**	**1.37 ± 0.071**	**1.23 ± 0.041**
Met-So/Met	0.023 ± 0.001	**0.045 ± 0.006**	0.032 ± 0.002	**0.026 ± 0.001**	**0.027 ± 0.003**
MUFA PC/SFA PC	3.46 ± 0.071	**4.91 ± 0.266**	**4.06 ± 0.119**	**3.70 ± 0.098**	**3.33 ± 0.077**
PC aa/PC ae	11.41 ± 0.288	**13.30 ± 0.441**	13.38 ± 0.335	12.23 ± 0.214	**11.91 ± 0.270**
BCAA/aromatic AA	1.30 ± 0.032	**1.71 ± 0.187**	**1.35 ± 0.034**	**1.31 ± 0.022**	**1.56 ± 0.049**

Note: All parameters are expressed as mean ± standard error of mean (SEM). Differences assessed by one-way ANOVA and Tukey's multiple comparison test; values in bold fonts, $p \leq 0.05$ for SuHx placebo compared to sham, for SuHx treatment groups compared to SuHx placebo.
NOX: normoxia control; SuHx: SU5416/hypoxia exposure; C16:1: hexadecenoyl-carnitine; C18:1: octadecenoyl-L-carnitine; ((C16 + C18)/C0): the ratio of hexadecanoyl-L-carnitine (C16) plus octadecanoyl-L-carnitine (C18) to L-Carnitine (C0); Ac-Orn: acetylornithine; lysoPC a C17:0: lysophosphatidylcholine acyl; lysoPC a C20:3: lysophosphatidylcholine acyl; lysoPC a C28:0: lysophosphatidylcholine acyl; PC aa C32:1: phosphatidylcholine diacyl C32:1; PC aa C34:1: phosphatidylcholine diacyl C34:1; PC aa C34:3: phosphatidylcholine diacyl C34:3; PC aa C36:1: phosphatidylcholine diacyl C36:1; PC aa C36:2: phosphatidylcholine diacyl C36:2; PC aa C36:3: phosphatidylcholine diacyl C36:3; PC ae C34:1: phosphatidylcholine acyl-alkyl C34:1; PC ae C36:1: phosphatidylcholine acyl-alkyl C36:1; PC ae C36:5: phosphatidylcholine acyl-alkyl C36:5; PC ae C38:4: phosphatidylcholine acyl-alkyl C38:4; PC ae C42:1: phosphatidylcholine acyl-alkyl C42:1; SM (OH) C14:1: hydroxysphingomyeline C14:1; Cit/Arg: citrulline to arginine ratio; Cit/Orn: citrulline to ornithine ratio; Met-So/Met: methioninesulfoxide (Met-SO) to methionine (Met) ratio; MUFA/SFA: monounsaturated fatty acids (MUFA) to saturated fatty acids (SFA) ratio; PC aa/PC ae: phosphatidylcholine diacyl (PC aa) to phosphatidylcholine acyl-alkyl (PC ae) ratio; BCAAs/AAAs: branched-chain amino acids (BCAAs) to aromatic amino acids (AAAs) ratio.

(ambrisentan[26] or macitentan[27]) where it attenuates PAH and RV remodeling in SuHx rats, or alone as demonstrated in multiple studies in MCT rats.[28–31] Of interest, tadalafil 10 mg/kg/day in rats is comparable to tadalafil 40 mg/day (the estimated highest clinical dose) in PAH patients, with an expected exposure level of 12,193 ng · h/mL in humans versus 12,600 ng· h/mL in rats.[28]

Like tadalafil, the dosing of macitentan also has been based on our acute hemodynamic study which indicates that 10 mg/kg induces an intermediate effect on pulmonary hemodynamics (−20 mmHg, data not shown). This also confirms the literature where chronic use of macitentan 10 mg/kg (four weeks) was found to be the lowest effective dose able to significantly attenuate RV hypertrophy in MCT rats.[13] Taken together, in rats, both agents were used at comparatively similar therapeutic doses.

Our study showed that despite of the absence of effects of monotherapies with either tadalafil or macitentan on PA remodeling, they markedly reduced RVSP. This may be explained by the presence and contribution of sustained pulmonary vasoconstriction to disturbed pulmonary hemodynamics in SuHx rats.[32] This suggests that the beneficial

(a)

(b)
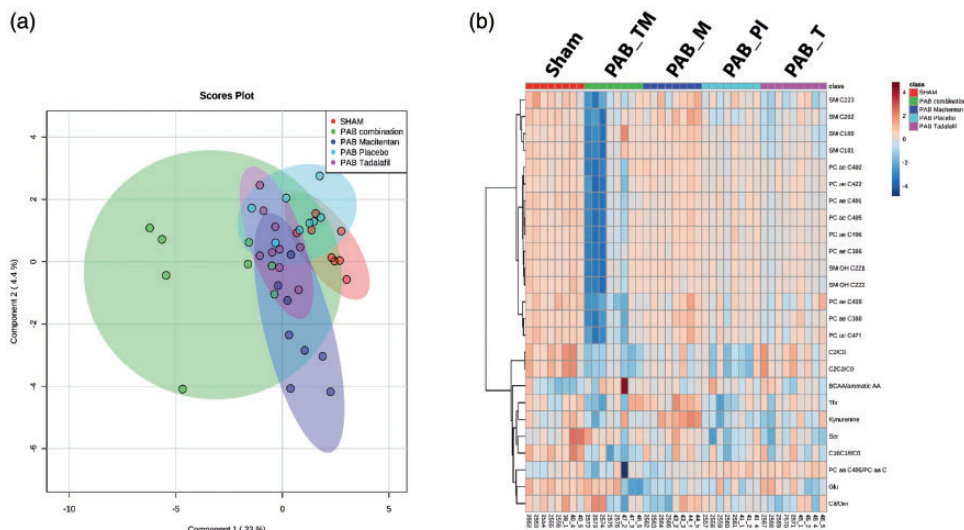
Fig. 6. Metabolomics profiling of plasma from PAB rats. (a) Metabolic profiling reveals only poor separation between plasma metabolite profiles from the different PAB rat groups by sparse partial least squares discriminant analysis. (b) Heat map of top 25 most altered metabolites by the model ordered by hierarchical clustering. Red represents high, and blue represents low abundance of the metabolite relative to the mean (white). Sham ($n = 8$); PAB: pulmonary artery banding; Pl: placebo ($n = 8$); T: tadalafil ($n = 9$); M: macitentan ($n = 8$); TM: combination of tadalafil and macitentan ($n = 8$).

Table 4. The most dysregulated metabolite ratios in PAB rats, and effects of tadalafil and macitentan and their combination on these ratios.

metabolite ratios N	Sham 8	PAB Placebo 8	PAB Tadalafil 9	PAB Macitentan 8	PAB combination 8
C2/C0	0.65 ± 0.018	$\mathbf{0.55 \pm 0.020}$	0.62 ± 0.016	0.58 ± 0.013	0.52 ± 0.012
(C2 + C3)/C0	0.68 ± 0.018	$\mathbf{0.57 \pm 0.020}$	$\mathbf{0.64 \pm 0.016}$	0.61 ± 0.011	0.55 ± 0.012
(C16 + C18)/C0	0.0055 ± 0.000	$\mathbf{0.0043 \pm 0.000}$	$\mathbf{0.0045 \pm 0.000}$	0.0048 ± 0.000	0.0039 ± 0.000

Note: All parameters are expressed as mean ± standard error of mean (SEM). Differences assessed by one-way ANOVA and Tukey's multiple comparison test; values in bold fonts, $p \leq 0.05$ for SuHx placebo compared to sham, for SuHx treatment groups compared to SuHx placebo.
PAB: pulmonary artery banding; ((C16 + C18)/C0): the ratio of hexadecanoyl-L-carnitine (C16) plus octadecanoyl-L-carnitine (C18) to L-Carnitine (C0); ((C2 + C3)/C0): the ratio of acetyl-L-carnitine (C2) plus propionyl-L-carnitine (C3) to L-carnitine (C0); C2/C0: the ratio of acetyl-L-carnitine (C2) to L-carnitine (C0).

effects of these agents alone or in combination may be mediated partly due to vasodilatory effects on sustained PA vasoconstriction rather than on PA remodeling.[33] Nevertheless, the anti-remodeling effects on PAs were also observed in SuHx rats treated with combination therapy, suggesting that to achieve reverse-remodeling effect on PAs at least two pathways involved in disease progression should be targeted. However, all therapies improved RV remodeling and function in parallel to the improvement of pulmonary hemodynamics in SuHx rats. Importantly, in SuHx rats, the most beneficial effects on the RV were seen with combination therapy, followed by macitentan and tadalafil monotherapy. Like SuHx rats, rats subjected to PAB surgery also displayed reduced CO compared to sham-operated counterparts. In addition, placebo PAB rats developed RV dysfunction and remodeling as shown by the measures of TAPSE, Fulton index, RVWT and

RVID. Previous studies have shown that PAB rats develop adaptive (compensated) RV remodeling compared to SuHx rats which develop maladaptive (decompensated) RV remodeling.[34] However, in rats, the development of maladaptive RV remodeling depends on the degree of RV pressure overload, and severe PA constriction in PAB model may lead to severe maladaptive (decompensated) RV remodeling.[35] In PAB rats, only macitentan exerted significant benefit on the RV. Although the combination therapy did not show beneficial effects on the RV in the PAB model, the results from the SuHx model indicate that the combination therapy had a strong effect on pulmonary hemodynamics generally. Taken together, in similar doses, both tadalafil and macitentan exert benefits to the RV with greater effect of the latter. Targeting two pathways with the combination of macitentan and tadalafil may be necessary to have reverse-remodeling effects on PA in SuHx rats.

In this study, we also analyzed circulating metabolites in both SuHx and PAB rat models. Initially, we searched for metabolites, which were significantly altered by disease versus healthy control and we investigated if the agents used were able to recover those changes in both SuHx and PAB rats. Evidence suggests that changed metabolism plays a key role in PAH pathogenesis[36] and a number of novel pharmacological agents targeting those changes are under investigation for their effects in PAH.[37] In addition, several circulating metabolites determine the adverse outcome of patients with PAH[38] serving as potential biomarkers. Moreover, some circulating metabolites are correlated with the RV parameters in PAH patients.[39] However, the effects of macitentan and tadalafil on plasma metabolites have not been studied completely. Our study revealed that SuHx-induced PAH in rats is associated with the changes in the plasma levels of acylcarnitines, amino acids, biogenic amines, phosphatidylcholines, lysophosphatidylcholines, and sphingophospholipid metabolisms which belong to arginine/proline, cysteine/methionine, aminoacyl-tRNA biosynthesis, sphingolipid, glutathione and glycerophospholipid metabolism pathways and therapies with tadalafil and macitentan alone or in combination similarly attenuated most of those changes. However, metabolic profiling with sPLS-DA indicates that the overall effect of macitentan and combination treatment was slightly stronger compared to tadalafil.

Among these altered metabolic changes in SuHx rats, citrulline metabolism was most pronounced. We found that the ratio of citrulline to both arginine (Cit/Arg) and ornithine (Cit/Orn) was increased in SuHx rats. Interestingly, all therapies equally attenuated those changes in SuHx rats. In the nitric oxide (NO) cycle, endothelial nitric oxide synthase (eNOS) metabolizes arginine to produce NO and citrulline as a by-product. The latter, can be recycled to arginine, again serving as a substrate for eNOS to NO synthesis.[40] NO plays an important role in maintaining pulmonary vascular homeostasis and disturbed NO production is associated with the development of PAH.[41] Utilization of arginine by arginase may also contribute to its decreased availability for eNOS. Arginase converts arginine to ornithine and urea and compete with eNOS for arginine.[42] Accordingly, increased arginase expression and activity contribute to the development/progression of PAH.[43,44] N-acetylornithine (Ac-Orn) is another circulating metabolite involved in the urea cycle, can be converted to ornithine, which is a precursor of citrulline in the urea cycle. Therefore, Ac-Orn can contribute to the refilling of the cellular citrulline pool to increase NO production by the NO cycle. SuHx rats display increased Ac-Orn levels, possibly as a compensatory reaction of the body to increase the availability of citrulline for the synthesis of NO. Interestingly, none of the therapies attenuated the changes in Ac-Orn levels.

Our study also revealed that SuHx rats display increased levels of long-chain fatty acyl carnitines (C16 and C18) and their ratio to free carnitine (C0). These changes may indicate reduced RV fatty acid metabolism of SuHx rats as previous studies have shown that PAH patients display increased levels of circulating long-chain fatty acyl carnitines[45,46] due to decreased RV fatty acid metabolism.[46] However, in contrast to SuHx rats, PAB rats displayed decreased ratios of short-chain (C2 and C3) as well as long-chain fatty acyl-carnitines (C16 and C18) to free carnitine (C0), which may indicate increased fatty acid utilization and metabolism. This discrepancy may be explained by the state of RV remodeling in these two models as PAB rats develop adaptive RV remodeling, while SuHx rats develop maladaptive RV remodeling. Since earlier studies have shown that adaptive RV remodeling is associated with activated RV metabolism and only transition to maladaptive RV remodeling is coupled with the reduced RV metabolism.[47,48]

In addition, our study also showed that several plasma phosphatidylcholines (PC) and lysophosphatidylcholine (lysoPC) species, which are major phospholipids in the circulation altered in SuHx rats but not in PAB rats. Left ventricular (LV) failure studies indicate that the disease pathogenesis is associated with the decreased levels of circulating phospholipids.[49–51] Our study revealed that SuHx rats display both increased (PC aa C32:1, PC aa C34:1, PC aa C36:1, PC aa C36:2, PC ae C34:1 and PC ae C36:1) as well as decreased PCs (PC ae C36:5, PC ae C38:4 and PC ae C42:1). Almost all changes in PC levels in SuHx rats were similarly attenuated with all therapies. However, currently the role of altered phospholipid metabolism in PAH pathogenesis and RV remodeling remains unknown.

Like PCs, three LysoPC species were changed in SuHx rats. Circulating LysoPC is mainly derived from phosphatidylcholine (PC) by the selective removal of one fatty acid residue by phospholipase A2 (PLA2). Currently, the role of lysoPCs in RV remodeling is not known. However, there are some insights from LV disease studies. For example, decreased level of circulating lysoPC C17:0 was associated with increased risk of myocardial infarction.[52] Similarly, lysoPC C17:0 decreased in SuHx rats, although, other two lysoPCs (lysoPC c20:3 and lysoPC C28:0) were increased. Therefore, the attenuation of lysoPC 17:0 levels by macitentan and combination treatment possibly reflects the observed improvement in RV remodeling in SuHx rats.

However, unlike to PAB model, the changes of circulating metabolites observed in SuHx rats cannot be exclusively attributed to the RV and may also be results of disturbed metabolism of the pulmonary vasculature as previous studies have shown that pulmonary vascular remodeling is associated with altered metabolism of the pulmonary vascular cells.[45,53–55] Interestingly, some of the altered metabolites we observed in this study have been found to involve in pulmonary vascular cellular dysfunction. For examples, dysregulation of acylcarnitine metabolism has been found to cause PAEC dysfunction[56] and phospholipid metabolism has been shown to mediate hypoxia-induced changes in

PAEC.[57] However, mechanistic studies are still lacking to link these changes to the specific pathologies of the pulmonary vasculature and RV remodeling.

Our study has several limitations which must be considered. Firstly, we used similar doses of tadalafil and macitentan based on our acute hemodynamic observation with a telemetry study (data not shown) and literature showing that both agents with similar doses equally reduce PAP in SuHx rats; however, it is known that in PAH patients the therapeutic dose of tadalafil is four times higher than that of macitentan (40 mg vs. 10 mg per day). Furthermore, only male animals were studied and the effects of those agents on the RV remodeling and plasma metabolites in female SuHx and PAB rats need to be addressed in the future studies. Moreover, we used only targeted metabolomics study which covers only limited number of metabolites and future studies with untargeted metabolomics may reveal more metabolites altered by the disease model. Lastly, we studied only plasma samples, and studying metabolite changes in the lung and RV tissues in addition to plasma samples may reveal more insights into the potential sources (lung vs. RV) of circulating metabolites.

Summary

In summary, both SuHx and PAB rats develop RV remodeling and dysfunction. SuHx rats display more pronounced circulating metabolomic changes, while PAB rats display modifications only in one metabolic pathway. Although, all therapies significantly attenuate SuHx-induced RV remodeling and dysfunction, the effects of macitentan are greater than tadalafil, while in PAB rats, only macitentan significantly improves RV remodeling and dysfunction. However, tadalafil and macitentan alone or in combination similarly attenuate majority of SuHx-induced metabolic changes, while only tadalafil could improve PAB-induced metabolic alterations. Taken together, metabolomic pathways may be dysregulated differently depending on the disease model and therefore the applied treatment strategies also may exert distinct effects on those changes. The findings of our study suggest that the beneficial effects of tadalafil and macitentan observed in various PAH models and PAH patients may be related to not only the improved pulmonary hemodynamics and RV function but also to their ability to modulate metabolomic changes.

Authors' contributions

RTS designed the study; AM, SZ, AS, BK, CV, AP, DK conducted the experiments; AM, SZ, AS, BK, JW, AP, DK, and RTS performed the data analysis; and AM, AW, SZ, AS, AP, DK and RTS wrote the manuscript HAG, FG, NW, WS IF, MI, SSP, and RTS critically revised the manuscript. All authors reviewed and revised the final version of manuscript and approved manuscript submission.

ORCID iDs

Argen Mamazhakypov https://orcid.org/0000-0002-2140-4819
Sven Zukunft https://orcid.org/0000-0002-1811-4562
Jochen Wilhelm https://orcid.org/0000-0001-5544-9647

Supplemental material

Supplemental material for this article is available online.

References

1. Schermuly RT, Ghofrani HA, Wilkins MR, et al. Mechanisms of disease: pulmonary arterial hypertension. *Nat Rev Cardiol* 2011; 8: 443–455.
2. Gomez-Arroyo J, Nikolic I and Yu PB. Animal models of pulmonary hypertension. In: Maron BA, Zamanian RT and Waxman AB (eds) *Pulmonary hypertension: basic science to clinical medicine*. Cham: Springer International Publishing, 2016, pp.161–172.
3. Maarman G, Lecour S, Butrous G, et al. A comprehensive review: the evolution of animal models in pulmonary hypertension research; are we there yet? *Pulmonary Circul* 2013; 3: 739–756.
4. Colvin KL and Yeager ME. Animal models of pulmonary hypertension: matching disease mechanisms to etiology of the human disease. *J Pulmonary Respir Med* 2014; 4: 198.
5. Lang M, Kojonazarov B, Tian X, et al. The soluble guanylate cyclase stimulator riociguat ameliorates pulmonary hypertension induced by hypoxia and SU5416 in rats. *PLoS One* 2012; 7: e43433.
6. Frump AL, Bonnet S, de Jesus Perez VA, et al. Emerging role of angiogenesis in adaptive and maladaptive right ventricular remodeling in pulmonary hypertension. *Am J Physiol Lung Cell Mol Physiol* 2018; 314: L443–l460.
7. Borgdorff MA, Dickinson MG, Berger RM, et al. Right ventricular failure due to chronic pressure load: what have we learned in animal models since the NIH working group statement? *Heart Fail Rev* 2015; 20: 475–491.
8. van de Veerdonk MC, Kind T, Marcus JT, et al. Progressive right ventricular dysfunction in patients with pulmonary arterial hypertension responding to therapy. *J Am Coll Cardiol* 2011; 58: 2511–2519.
9. Galiè N, Humbert M, Vachiery J-L, et al. 2015 ESC/ERS guidelines for the diagnosis and treatment of pulmonary hypertension: the Joint Task Force for the Diagnosis and Treatment of Pulmonary Hypertension of the European

Society of Cardiology (ESC) and the European Respiratory Society (ERS): endorsed by: Association for European Paediatric and Congenital Cardiology (AEPC), International Society for Heart and Lung Transplantation (ISHLT). *European heart journal* 2015; 37: 67–119.

10. Sitbon O and Gaine S. Beyond a single pathway: combination therapy in pulmonary arterial hypertension. *Eur Respir Rev* 2016; 25: 408–417.

11. Viswanathan G, Mamazhakypov A, Schermuly RT, et al. The role of G Protein-coupled receptors in the right ventricle in pulmonary hypertension. *Front Cardiovasc Medo* 2018. DOI: 10.3389/fcvm.2018.00179.

12. Bolli MH, Boss C, Binkert C, et al. The discovery of N-[5-(4-bromophenyl)-6-[2-[(5-bromo-2-pyrimidinyl) oxy] ethoxy]-4-pyrimidinyl]-N′-propylsulfamide (macitentan), an orally active, potent dual endothelin receptor antagonist. *J Med Chem* 2012; 55: 7849–7861.

13. Iglarz M, Binkert C, Morrison K, et al. Pharmacology of macitentan, an orally active tissue-targeting dual endothelin receptor antagonist. *J Pharmacol Exp Ther* 2008; 327: 736–745.

14. Pulido T, Adzerikho I, Channick RN, et al. Macitentan and morbidity and mortality in pulmonary arterial hypertension. *N Engl J Med* 2013; 369: 809–818.

15. Rosenkranz S, Galiè N, Channick R, et al. Effects of macitentan on right ventricular remodeling in pulmonary arterial hypertension: results from the REPAIR study interim analysis. *J Am Coll Cardiol* 2019; 73: 1898.

16. Mercurio V, Mukherjee M, Tedford RJ, et al. Improvement in right ventricular strain with ambrisentan and tadalafil upfront therapy in scleroderma-associated pulmonary arterial hypertension. *Am J Resp Crit Care* 2018; 197: 388–391.

17. van de Veerdonk MC, Marcus JT, Westerhof N, et al. Upfront combination therapy reduces right ventricular volumes in pulmonary arterial hypertension. *Eur Respir J* 2017; 49: 1700007.

18. Rain S, Handoko M, Noordegraaf AV, et al. Pressure-over-load-induced right heart failure. *Pflügers Archiv Eur J Physiol* 2014; 466: 1055–1063.

19. Archer SL, Fang Y-H, Ryan JJ, et al. Metabolism and bio-energetics in the right ventricle and pulmonary vasculature in pulmonary hypertension. *Pulmonary Circul* 2013; 3: 144–152.

20. Rhodes CJ, Ghataorhe P, Wharton J, et al. Plasma metabolomics implicates modified transfer RNAs and altered bioenergetics in the outcomes of pulmonary arterial hypertension. *Circulation* 2017; 135: 460–475.

21. Kilkenny C, Browne W, Cuthill IC, et al. Animal research: reporting in vivo experiments: the ARRIVE guidelines. *Br J Pharmacol* 2010; 160: 1577–1579.

22. Savai R, Al-Tamari HM, Sedding D, et al. Pro-proliferative and inflammatory signaling converge on FoxO1 transcription factor in pulmonary hypertension. *Nat Med* 2014; 20: 1289–1300.

23. Cheng HW, Fisch S, Cheng S, et al. Assessment of right ventricular structure and function in mouse model of pulmonary artery constriction by transthoracic echocardiography. *J Visual Exp* 2014; 84: e51041.

24. Weisel FC, Kloepping C, Pichl A, et al. Impact of S-adenosyl-methionine decarboxylase 1 on pulmonary vascular remodeling. *Circulation* 2014; 129: 1510–1523.

25. Zukunft S, Prehn C, Röhring C, et al. High-throughput extraction and quantification method for targeted metabolomics in murine tissues. *Metabolomics* 2018; 14: 18.

26. Aiello RJ, Bourassa P-A, Zhang Q, et al. Tryptophan hydroxylase 1 inhibition impacts pulmonary vascular remodeling in two rat models of pulmonary hypertension. *J Pharmacol Exp Ther* 2017; 360: 267–279.

27. Boucherat O, Chabot S, Paulin R, et al. HDAC6: a novel histone deacetylase implicated in pulmonary arterial hypertension. *Sci Rep* 2017; 7: 4546.

28. Sawamura F, Kato M, Fujita K, et al. Tadalafil, a long-acting inhibitor of PDE5, improves pulmonary hemodynamics and survival rate of monocrotaline-induced pulmonary artery hypertension in rats. *J Pharmacol Sci* 2009; 111: 235–243.

29. Zhang W-H, Liu C-P, Zhang Y-J, et al. Additive effect of tadalafil and simvastatin on monocrotaline-induced pulmonary hypertension rats. *Scand Cardiovasc J* 2012; 46: 374–380.

30. Leong ZP and Hikasa Y. Effects of masitinib compared with tadalafil for the treatment of monocrotaline-induced pulmonary arterial hypertension in rats. *Vasc Pharmacol* 2019; Nov-Dec: 122123: 106599.

31. Egawa M, Ishikura F, Nishikawa R, et al. Effects of tadalafil to prevent thickening of pulmonary artery in monocrotaline-induced pulmonary hypertension rats: compared with echocardiographic findings. *J Hypertension* 2010; 28: e196–e197.

32. de Raaf MA, Schalij I, Gomez-Arroyo J, et al. SuHx rat model: partly reversible pulmonary hypertension and progressive intima obstruction. *Eur Resp J* 2014; 44: 160–168.

33. Hoenicka M, Golovchenko S, Englert L, et al. Combination therapy of pulmonary arterial hypertension with vardenafil and macitentan assessed in a human ex vivo model. *Cardiovasc Drugs Ther* 2019; 33: 1–9.

34. Bogaard HJ, Natarajan R, Henderson SC, et al. Chronic pulmonary artery pressure elevation is insufficient to explain right heart failure. *Circulation* 2009; 120: 1951–1960.

35. Andersen S, Schultz JG, Holmboe S, et al. A pulmonary trunk banding model of pressure overload induced right ventricular hypertrophy and failure. *J Visual Exp* 2018; 141: e58050.

36. Frump AL and Lahm T. The basic science of metabolism in pulmonary arterial hypertension. *Adv Pulmonary Hypertension* 2018; 17: 95–102.

37. Brittain EL. Clinical trials targeting metabolism in pulmonary arterial hypertension. *Adv Pulmonary Hypertension* 2018; 17: 110–114.

38. Rhodes CJ, Ghataorhe P, Wharton J, et al. Plasma metabolomics implicate modified transfer RNAs and altered bioenergetics in the outcome of pulmonary arterial hypertension. *Circulation* 2016; 135: 460–475.

39. Attard MI, Dawes TJ, de Marvao A, et al. Metabolic pathways associated with right ventricular adaptation to pulmonary hypertension: 3D analysis of cardiac magnetic resonance imaging. *Eur Heart J* 2018; 20: 668–676.

40. Solomonson LP, Flam BR, Pendleton LC, et al. The caveolar nitric oxide synthase/arginine regeneration system for NO production in endothelial cells. *J Exp Biol* 2003; 206: 2083–2087.

41. Chester AH, Yacoub MH and Moncada S. Nitric oxide and pulmonary arterial hypertension. *Global Cardiol Sci Pract* 2017; 2017: 14–14.

42. Maarsingh H, Pera T and Meurs H. Arginase and pulmonary diseases. *Naunyn Schmiedebergs Arch Pharmacol* 2008; 378: 171–184.

43. Zheng H-K, Zhao J-H, Yan Y, et al. Metabolic reprogramming of the urea cycle pathway in experimental pulmonary

arterial hypertension rats induced by monocrotaline. *Respir Res* 2018; 19: 94.

44. Cowburn AS, Crosby A, Macias D, et al. HIF2α–arginase axis is essential for the development of pulmonary hypertension. *Proc Natl Acad Sci U S A* 2016; 113: 8801–8806.

45. Luo N, Craig D, Ilkayeva O, et al. Plasma acylcarnitines are associated with pulmonary hypertension. *Pulmonary Circ* 2017; 7: 211–218.

46. Brittain EL, Talati M, Fessel JP, et al. Fatty acid metabolic defects and right ventricular lipotoxicity in human pulmonary arterial hypertension. *Circulation* 2016; 133: 1936–1944.

47. Sutendra G, Dromparis P, Paulin R, et al. A metabolic remodeling in right ventricular hypertrophy is associated with decreased angiogenesis and a transition from a compensated to a decompensated state in pulmonary hypertension. *J Mol Med* 2013; 91: 1315–1327.

48. Paulin R, Sutendra G, Gurtu V, et al. A miR-208–Mef2 axis drives the decompensation of right ventricular function in pulmonary hypertension. *Circul Res* 2015; 116: 56–69.

49. Kärkkäinen O, Tuomainen T, Mutikainen M, et al. Heart specific PGC-1α deletion identifies metabolome of cardiac restricted metabolic heart failure. *Cardiovasc Res* 2018; 115: 107–118.

50. Sansbury BE, DeMartino AM, Xie Z, et al. Metabolomic analysis of pressure-overloaded and infarcted mouse hearts. *Circulation* 2014; 7: 634–642.

51. Cheng M-L, Wang C-H, Shiao M-S, et al. Metabolic disturbances identified in plasma are associated with outcomes in patients with heart failure: diagnostic and prognostic value of metabolomics. *J Am Coll Cardiol* 2015; 65: 1509–1520.

52. Ward-Caviness CK, Xu T, Aspelund T, et al. Improvement of myocardial infarction risk prediction via inflammation-associated metabolite biomarkers. *Heart* 2017; 103: 1278–1285.

53. Hemnes AR, Luther JM, Rhodes CJ, et al. Human PAH is characterized by a pattern of lipid-related insulin resistance. *JCI Insight* 2019; 4: e123611.

54. Chouvarine P, Giera M, Kastenmüller G, et al. Trans-right ventricle and transpulmonary metabolite gradients in human pulmonary arterial hypertension. *Heart* 2020; 21(4): 340–349.

55. Rafikova O, Meadows ML, Kinchen JM, et al. Metabolic changes precede the development of pulmonary hypertension in the monocrotaline exposed rat lung. *PLoS One* 2016; 11: e0150480.

56. Sharma S, Sud N, Wiseman DA, et al. Altered carnitine homeostasis is associated with decreased mitochondrial function and altered nitric oxide signaling in lambs with pulmonary hypertension. *Am J Physiol Lung Cell Mol Physiol* 2008; 294: L46–56.

57. Bhat GB and Block ER. Effect of hypoxia on phospholipid metabolism in porcine pulmonary artery endothelial cells. *Am J Physiol* 1992; 262: L606–L613.